Toward Phase-Variable Control of Sit-to-Stand Motion with a Powered Knee-Ankle Prosthesis

Daphna Raz[1], Edgar Bolívar-Nieto[1], Necmiye Ozay[1,2], and Robert D. Gregg[1,2]

***Abstract*— This paper presents a new model and phase-variable controller for sit-to-stand motion in above-knee amputees. The model captures the effect of work done by the sound side and residual limb on the prosthesis, while modeling only the prosthetic knee and ankle with a healthy hip joint that connects the thigh to the torso. The controller is parametrized by a biomechanical phase variable rather than time and is analyzed in simulation using the model. We show that this controller performs well with minimal tuning, under a range of realistic initial conditions and biological parameters such as height and body mass. The controller generates kinematic trajectories that are comparable to experimentally observed trajectories in non-amputees. Furthermore, the torques commanded by the controller are consistent with torque profiles and peak values of normative human sit-to-stand motion. Rise times measured in simulation and in non-amputee experiments are also similar. Finally, we compare the presented controller with a baseline proportional-derivative controller demonstrating the advantages of the phase-based design over a set-point based design.**

I. Introduction

The sit-to-stand motion is an essential part of everyday life, performed an average of 60 times per day by healthy adults [1]. Although able-bodied individuals may execute this movement with ease, sit-to-stand presents a challenge to those with impaired mobility. Compared to other common tasks such as walking and stair climbing, sit-to-stand requires high torques, particularly at the knee [2]. Furthermore, loss of balance can occur during the transition from the seated position, where the basin of stability is relatively large, to the more unstable standing position [3]. Such failures may involve taking a step or having to sit back down [4].

Unilateral amputees present a special case of impaired mobility, due to the asymmetry in joint torques they exhibit between the sound and amputated sides [5]. Passive prostheses are a source of this asymmetry, as they cannot perform net positive work like the intact leg. The sound side must compensate for the lack of assistance on the amputated side via the production of even higher torques [6], which can, in turn, lead to physiological asymmetries in the muscles and joints [7].

[1]Robotics Institute, University of Michigan, Ann Arbor, MI 48109, USA. {daphraz,ebolivar}@umich.edu

[2]Electrical and Computer Engineering, University of Michigan, Ann Arbor, MI 48109, USA. {necmiye,rdgregg}@umich.edu

This work was supported by the National Institute of Child Health & Human Development of the NIH under Award Number R01HD094772. This work was also supported by NSF Awards 1949346, 2024237, and 1553873. The content is solely the responsibility of the authors and does not necessarily represent the official views of the NIH or NSF.

Recent powered knee-ankle prostheses are capable of producing enough torque to assist meaningfully during sit-to-stand [8], [9]. Sit-to-stand controllers for these types of legs have primarily used impedance-based approaches [10], [11]. Typically, joint mechanics are modeled and controlled as a spring-damper system, where the stiffness, viscosity, and equilibrium angle are held constant within discrete phases of a finite state machine for a given task [10], [11]. In the first example [10], a non-smooth knee angle vs. stiffness curve was tuned based on subject preference. The results show that the controller commanded non-smooth torques. In [11] researchers used the impedance control framework, but the desired stiffness curves for sit-to-stand were parameterized as linear functions of the measured axial force along the prosthesis. This parameterization implicitly depends on the user evenly loading both legs, and the parametrizing signal can be lost instantaneously if the subject removes their weight from the amputated side. Indeed, significant improvements in load-bearing symmetry were only measured in the first half of the sit-to-stand motion. These impedance-based control methods also tend to require extensive subject-specific tuning of their many parameters [12].

Phase variable control methods offer some advantages over these conventional impedance-based methods. Desired kinematic patterns are parametrized as a function of a monotonic biomechanical phase variable, such as thigh angle [13]–[15], which represents progression through the task cycle. These functions can be learned from experimental data [14]. If the desired function and phase variable are continuously differentiable, then a control law can be designed with desirable smoothness properties. Typically, phase variables do not depend on subject-specific parameters such as weight and height [13]. Furthermore, a thigh-based phase variable is easily measured from an inertial measurement unit mounted on the prosthetic knee joint and is directly actuated by the amputee's intact hip joint [15]. This allows for indirect volitional control of the prosthesis, whereby the user adjusts the thigh angle to drive desired motion in the prosthetic leg, including forward and backward progression [14]. However, this phase-based control framework has not yet been used for sit-to-stand motion.

A further gap in the literature exists in the mathematical modeling of sit-to-stand motion for amputees. Prior controllers have been validated directly in human subject studies [11], but sometimes with only one participant [10]. While experimentally validating a controller is vitally important, mathematical models provide a way to study a controller's behavior safely in simulation under multiple conditions (e.g.,

initial conditions or subject parameters), before putting a human user at risk. Unlike amputee sit-to-stand, non-amputee sit-to-stand has been modeled extensively [16]. Existing models typically represent the human as a planar three-link serial chain with torque inputs representing the ankle, knee, and hip joints [17], or as a full five-link model that includes left and right legs attached to a torso [18]. Some models of even higher dimension incorporate the foot and muscle dynamics [19]. These models present several challenges for analyzing controllers for powered prostheses. A three-link model of the amputated side that is only actuated at those joints cannot replicate the distinct contribution of the sound side and of the muscles of the residual limb. For example, amputees could initiate a sit-to-stand motion by applying torques only from their intact joints, which in turn would alter the prosthetic leg angles without direct actuation. This asymmetry could not be manifested in the three-link model. A five-link model, on the other hand, can be used to represent the full body dynamics and the effect of the sound side. However, a fully actuated five-link model will consist of ten dimensions, at a minimum, and would require the design of a distinct, biomimetic sound-side controller.

This paper introduces two contributions. We first present a new, low-dimensional model of an above-knee amputee during sit-to-stand, in which full lower-body behavior is approximated with a three-link model and a lumped sound-side and residual limb force input. We then introduce a phase-variable controller for sit-to-stand motion, and use our model to analyze its performance. We improve on prior work in [10] and [11] by defining an explicit control law that is inspired by human biomechanics and is invariant to subject parameters. Our controller gains are consistent across subjects. We use the thigh angle as a phase variable, which is less sensitive to leg loading with the ground. We validate that this controller produces ankle and knee angle kinematic trajectories that are similar to able-bodied trajectories in a previously collected dataset [20]. The torque and power profiles are smooth and comparable to non-amputee profiles during sit-to-stand. Rise times measured in simulation fall well within the range of rise times recorded in non-amputee experiments. We demonstrate several advantages of our phase-variable method through comparisons with a simplified impedance-based method, specifically using a proportional-derivative controller with a constant set-point.

II. Preliminaries

A. The Sit-to-Stand Movement

Normative sit-to-stand in able-bodied humans can be divided into five or more distinct phases, with the transition between different phases being marked by peak angles or velocities in various joints [21]. In this paper, we refer to the simplified model in [22], which considers three phases of motion. After quiet sitting, the subject tilts their torso forward during the first phase of motion, *preparation*. The second phase, *ascent*, begins when the subject is no longer in contact with chair. During this phase, the subject rises to a standing position. Full standing can be defined based on the full extension of the joints, or the location of the center of mass [22]. Once the subject is standing, the third phase consists of *stabilization* during standing. A graphical depiction of the phases of motion can be seen in Figure 1.

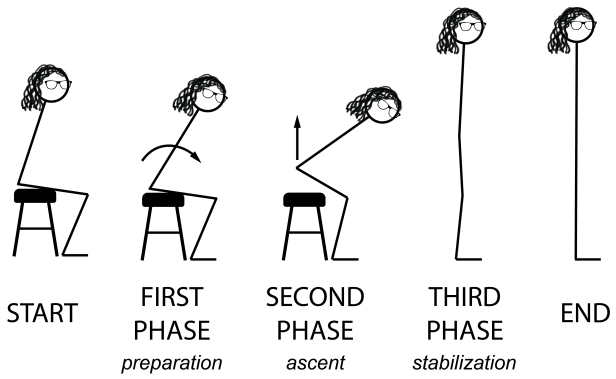

Fig. 1. Depiction of the three phases of the sit-to-stand movement. Figure adapted from [22].

In the simulations presented in the following sections, we consider only the ascent phase, as this is the phase of motion during which positive work must be done by the prosthesis. Preparation and stabilization depend highly on torso motion, which we do not control.

B. Experimental Data

The data used in the controller design and analysis come from [20]. This dataset consists of the lower-limb measurements of ten able-bodied subjects performing a variety of tasks, including sit-to-stand and stand-to-sit. Subjects were aged $20 - 60$ years (30.4 ± 14.9), weighed 74.6 ± 9.7 kg, and had an average height of 1.73 ± 0.09 meters. The measurements consist of pelvic tilt, hip, knee, and relative ankle joint angles, and force plate measurements.

For sit-to-stand, subjects sat on a backless stool. Each subject performed six trials which consisted of rising from the stool, standing at rest for a beat, and returning to sitting. Subjects were instructed not to use their hands for assistance during transitions.

III. Model

Anatomical models are generally reduced to link-segment models in biomechanical analysis [23], with the choice of the number of links depending on the task to be modeled. Explicitly representing the differing joint torques of the sound and amputated side requires a five-link model, with links corresponding to the Head-Arms-Trunk (HAT) segment and the left and right thigh and shank segments. Under a pinned foot assumption, this becomes a closed and parallel kinematic chain. Thus the same trajectory for sit-to-stand can be produced under a continuous range of loading conditions between the sound and amputated side, including loading of only the sound side.

To approximate the parallel behavior of the five-link model in a lower dimensional manner, we model the torso with only the amputated side as a planar three-link kinematic

chain. Note that in our angle convention, positive knee torque matches knee flexion and positive ankle torque is equal to ankle dorsiflexion.

Throughout the ascent phase of sit-to-stand, acceleration of the center of mass in the vertical direction is approximately constant after an initial overshoot, while the acceleration in the horizontal direction is negligible [24]. To match this behavior, we introduce a constant vertical force at the center of mass of the torso link that serves three main purposes: representing the assistance provided by the healthy side and residual limb musculature to the amputated side, initiating sit-to-stand motion, and pulling the torso into its final vertical position at the end of the sit-to-stand motion. The need to separately model and control the joints of the sound-side knee, ankle, and hip is eliminated.

As shown in Figure 2, θ_1, θ_2, θ_3, and s correspond to the ankle, knee, hip, and thigh angle, respectively. The prosthesis actuates θ_1 and θ_2 directly, represented by torques u_1 and u_2. We augment the standard form of the equations of motion for a three-link planar arm, derived via the system Lagrangian [25]:

$$M(\theta)\ddot{\theta} + C(\theta,\dot{\theta})\dot{\theta} + N(\theta) = u + J_B^T \cdot Ad_{V\to B} \cdot F. \quad (1)$$

Here, $\theta = \begin{bmatrix}\theta_1 & \theta_2 & \theta_3\end{bmatrix}^T$ is the vector of joint positions, $M(\theta)$ is the position-dependent inertia matrix, $C(\theta,\dot{\theta})$ is the Coriolis matrix, $N(\theta)$ consists of torques due to gravity, and $u = \begin{bmatrix}u_1 & u_2 & 0\end{bmatrix}^T$ is a vector of control inputs from the prosthesis. Note that the last component of u is 0, as the hip angle, θ_3, is not actuated by the prosthesis.

The vertical force is represented as a wrench $F = \begin{bmatrix}f_x & f_y & \tau\end{bmatrix}^T$, which is attached to frame V. The origin of V is the center of mass of the third link, and its orientation is aligned with the global frame G. The first two coordinates of the wrench F represent the forces applied along the x and y axes and the third coordinate represents the torque applied about the axis passing through the origin of V. As we are only using a constant vertical force to assist with sit-to-stand motion, the second coordinate of F will be a constant, while the other coordinates will be zero.

The matrix $Ad_{V\to B}$ represents the adjoint transformation which transforms wrench coordinates of frame V into coordinates in frame B, the link frame attached to the center of mass of the torso. The applied force is then mapped to joint torques via the body Jacobian, J_B^T. A detailed description of wrenches and the body Jacobian can be found in [25].

The constant vertical force along the y-axis approximates the sound side and residual limb function of raising the body's center of mass during the sit-to-stand task. The force can be reduced to simulate loading on the sound side that raises the torso and initiates movement, but does not fully rise to a full standing position without additional actuation.

IV. CONTROLLER DESIGN

Prior work in legged robotics has used virtual constraints based on holonomic phase variables to produce time-invariant joint trajectories [26]. This work has been successfully extended to walking controllers for powered prosthetic legs [14]. Here, we use the thigh angle to define a holonomic phase variable, s. The kinematic model, including s, can be seen in Figure 2. A key benefit of selecting the thigh angle is that its value monotonically decreases during sit-to-stand, as shown in Figure 3. This phase variable can be easily measured in real time using an Inertial Measurement Unit mounted to top of the prosthesis knee joint hinge, giving the prosthesis socket orientation [9]. We approximate a nominal relationship between the phase variable and the knee angle, which we denote $h(s)$, using insight gleaned from human subject data, which we show in Section IV-A. Given the kinematic constraints of our model, we express a nominal relationship between s and the ankle angle that depends linearly on s and $h(s)$. We define our desired angles based on these nominal relationships, which we enforce using a proportional-derivative controller on error dynamics in Section IV-B.

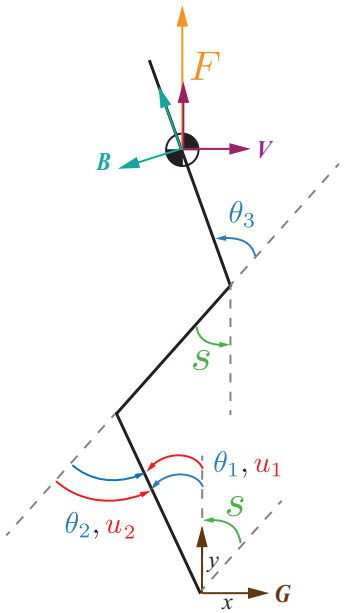

Fig. 2. Three link model of the prosthesis side of a person with amputation performing sit-to-stand. θ_1, θ_2, θ_3, and s correspond to the ankle, knee, hip, and thigh angle, respectively F denotes the approximation of the effects of the sound side, and u_1 and u_2 denote the prosthesis controller inputs. Under this angle convention, positive knee torque matches knee flexion and positive ankle torque is equal to ankle dorsiflexion. The relationship between s, θ_1, and θ_2 is illustrated in the bottom third of the figure.

A. Design of Kinematic Constraints

The ankle angle θ_1 can be expressed as a function of the phase variable s and knee angle θ_2 by

$$\theta_1 = -\theta_2 - s. \quad (2)$$

This relationship can be seen in Figure 2. Given this simple linear relationship, it suffices to compute a map from s to a desired knee angle

$$\theta_2^{des} = h(s). \quad (3)$$

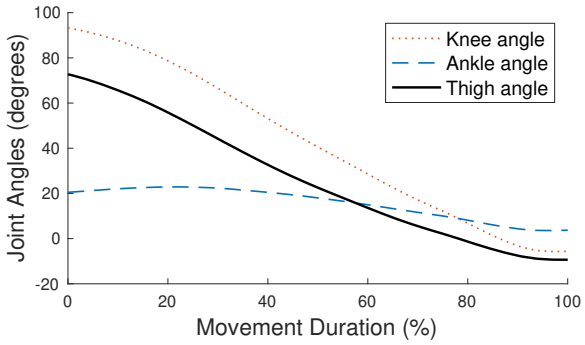

Fig. 3. Normative sit-to-stand kinematics measured in an able-bodied subject. The thigh angle decreases monotonically, making it suitable to be used as a phase variable.

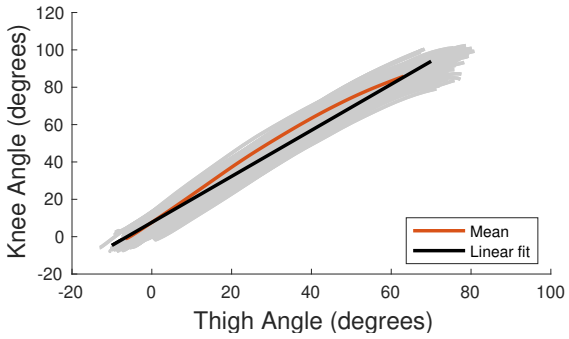

Fig. 4. Plot of sit-to-stand data collected from non-amputees. Individual trials are plotted in gray, while the computed nominal trajectory (mean) is in red. The line of best fit is in black. RMSE for this linear fit was $4.03°$.

The desired ankle angle can then be obtained from (2):

$$\theta_1^{des} = -h(s) - s. \tag{4}$$

Although we do not model the foot, in practice (4) will have the effect of keeping the foot flat on the ground. Several approaches can be taken for designing $h(s)$, which should represent the natural biomechanics of the thigh-knee relationship. One option is to compute nominal thigh-knee trajectories from large enough data sets, fitting a Bezier polynomial to the result. However, data from the dataset in Section II indicate that in the case of sit-to-stand motion, the thigh and knee angles exhibit a proportional relationship as long as the human's foot remains on the ground. In our simplified model, the pinned foot constraint guarantees this relationship. Analysis of data from human trials confirms that it is realistic to assume both a linear mapping from thigh angle to knee, and a pinned foot.

The thigh angle vs. knee angle from all trials of all subjects for sit-to-stand are shown in Figure 4. A linear fit was computed using linear least squares over these trials. The nominal trajectory for a virtual constraint controller consists of the average of all trials at each timestep. The RMSE between the linear fit and the nominal trajectory is $4.03°$. Thus the data show that the thigh vs. knee relationship is well approximated by a linear model.

Observing this linear relationship, we assume that $h(s)$, which determines our desired knee angle, takes the form

$$h(s) = c_1 s + c_2 \tag{5}$$

for the parameter vector $c = \begin{bmatrix} c_1 & c_2 \end{bmatrix}^T \in \mathbb{R}^2$.

For an individual subject, $h(s)$ can be computed at motion onset using the initial thigh angle s_0, and the initial knee angle $\theta_{2,0}$, with the assumption that $s_f = 0$ and $\theta_{2,f} = 0$ which indicates standing at full knee extension. We compute the parameters of the line connecting the initial and final point by solving

$$\begin{bmatrix} s_0 & 1 \\ s_f & 1 \end{bmatrix} c = \begin{bmatrix} \theta_{2,0} \\ \theta_{2,f} \end{bmatrix}. \tag{6}$$

for the parameter vector c.

B. Controller

We substitute equation (5) into equations (3) and (4) and construct a feedback controller with the desired position determined by $h(s)$. The position error for the knee, or θ_2, becomes

$$e_2 = h(s) - \theta_2 \tag{7}$$

and the derivative of the error is

$$\dot{e}_2 = \dot{h}(s) - \dot{\theta}_2. \tag{8}$$

The error term e_1 corresponding to θ_1 is computed similarly. A proportional-derivative control law is then used to command the knee and ankle motor torque at each joint $i \in \{1, 2\}$:

$$u_i = K_{p_i} e_i + K_{d_i} \dot{e}_i \tag{9}$$

where $K_{p_i} > 0$ and $K_{d_i} > 0$ are proportional and derivative gains, respectively.

V. Simulation Results

To analyze the performance of the phase-variable controller under realistic parameters and initial conditions, we refer to the dataset described in Section II-B. The parameters of the three-link model (masses and link lengths) were matched to the parameters of the ten subjects in the dataset, shown in Table I. We assume that the prosthesis is height-adjustable, such that the prosthesis shank length and socket connection approximate the length of the subject's sound leg. Thus the link lengths were computed based on the subject's total height, and distributed based on cadaver data studies [27]. Mass was distributed similarly for the thigh and HAT segment, while the shank was modeled to match a powered prosthesis weighing 4 kg [8].

For the phase-variable controller (PV), the same gains were used for all subjects, with $K_{p_1} = 500$, $K_{p_2} = 1000$, $K_{d_1} = 250$, $K_{d_2} = 400$. To benchmark the controller, we also implemented a set-point proportional-derivative controller (SP),

$$u_i = K_{p,i}(\theta_{d,i} - \theta_i) - K_{d,i}\dot{\theta}_i, \tag{10}$$

with the desired set-point, θ_d, set to the standing configuration at zero velocity. The same gains were used for all

subjects, with $K_{p_1} = 75$, $K_{p_2} = 150$, $K_{d_1} = 30$, $K_{d_2} = 60$. The gains were tuned to mitigate overly aggressive rise times. For both controllers, the magnitude of the vertical force was set as 90% of the total mass of the model times gravitational acceleration; this is sufficient to initiate sit-to-stand motion and maintain an upright torso, while still requiring actuation from the prosthesis to rise fully to standing.

For each of the six sit-to-stand trials performed by each subject in the experiment, we mapped the subject's height, weight, and initial limb configuration (ankle, knee, and hip angle) to the three link model. We ran a simulation starting from that configuration, providing the PV controller inputs and constant vertical force inputs as described in Section III. We then repeated the trial using the SP controller.

A. Torque and Power Profiles

The commanded prosthesis torques with the phase-variable controller are shown in Figure 5. As joint torques were not yet available from [20], we compare to normative reference curves generated from ten-able bodied subjects performing sit-to-stand in [28].

The magnitude of the peak mean torque in the ankle joint is 0.25 $\mathrm{Nm/kg}$ with the phase-variable controller. This is slightly lower than the peak mean torque magnitude of 0.45 $\mathrm{Nm/kg}$ observed in [28]. The magnitude of the mean peak torque in the simulated prosthetic knee joint is 0.42 $\mathrm{Nm/kg}$. Like the ankle, this is lower than the peak mean torque magnitude of 0.82 $\mathrm{Nm/kg}$ in [28]. In the simulation, peak ankle torque is 60% of peak knee torque, quite close to the 62% found in [28]. The peak knee torques occur at 5% and 13% of motion, respectively.

Peak torque magnitude can be increased as desired via tuning of the controller gains. However, we note that chair height, subject limb length, and subject limb mass affect loading during sit-to-stand [29], so absolute numbers from various studies can only serve as a rough guide. These factors contribute to the variability observed in the phase-variable controller. Importantly, the knee torque smoothly rises to its peak directly after the initiation of ascent, similar to the normative curve. These results bode well for the phase-variable controller's ability to produce torques symmetrical to the sound side, enabling loading of the amputated side.

In contrast, the SP controller lacks the smooth profile of the phase-variable controller, with torques shown in Figure 6. The SP controller results in a peak mean torque magnitude of 4.5 $\mathrm{Nm/kg}$ in the knee, which is far beyond values observed in able-bodied human studies [24], [28]. Peak mean ankle torque is 0.51 $\mathrm{Nm/kg}$, and is only 11% of the knee torque.

The power generated by the prosthesis at the knee and ankle joints (mostly positive) is shown in Figure 5. For comparison, the power generated by the SP controller is shown in Figure 6. The peak power for the PV controller at the knee is $0.46\,\mathrm{W\,kg^{-1}}$ at 15% of movement duration, which corresponds to the mean peak power of $0.9\,\mathrm{W\,kg^{-1}}$ at $23\,\%$ in [28]. The peak power for the PV controller at the ankle is $0.06\,\mathrm{W\,kg^{-1}}$ which corresponds to the mean peak power of $0.19\,\mathrm{W\,kg^{-1}}$ for able-bodied subjects in [28]. As with torque, the peak knee power of the SP controller is excessive ($4.1\,\mathrm{W\,kg^{-1}}$).

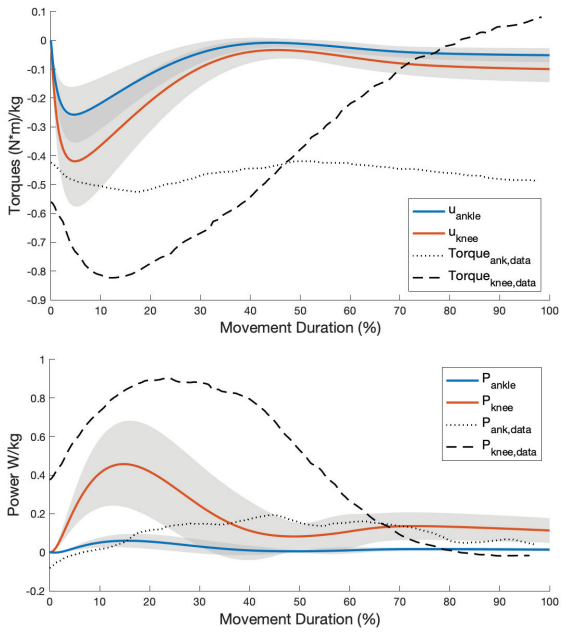

Fig. 5. Mean torques and powers from the phase-variable controller (PV) for both the knee and ankle, with normative reference curves from a human subject dataset [28]. The dataset includes an unexplained torque offset at standing in the ankle torque. The gray shaded area spans $\pm$ one standard deviation across simulated trials.

TABLE I
SUBJECT PARAMETERS

Subject	Height (m)	Weight (kg)
1	1.90	87.0
2	1.74	75.0
3	1.62	61.4
4	1.80	77.5
5	1.64	77.4
6	1.77	73.3
7	1.62	53.7
8	1.81	85.1
9	1.77	81.2
10	1.62	74.7

B. Comparing Prosthesis Kinematics to Human Data

Here, we compare each simulated trial to the corresponding sit-to-stand trial in the dataset starting from the same initial condition, with the same parameters. We compute the RMSE between the simulated sit-to-stand kinematics with the PV controller and the kinematics measured in the experiment. We repeat this comparison using the SP controller. For each controller and subject, we average the RMSE results across trials. These results are reported in the second and third columns of Table II for the PV controller, and the fourth and fifth columns for the SP controller. Figure 7 shows a representative experimental trial compared to the corresponding PV and SP simulations.

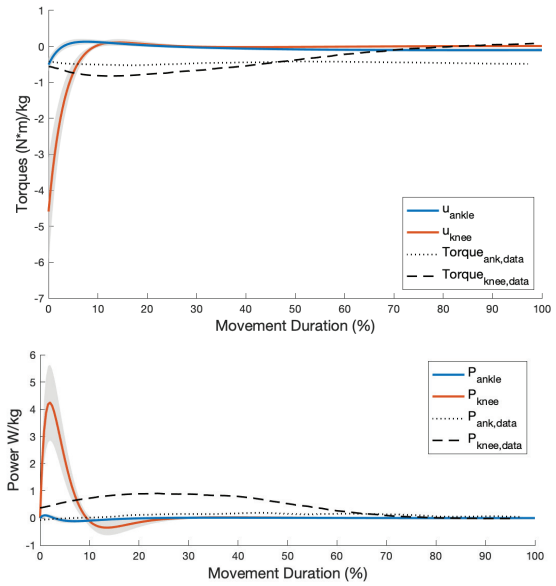

Fig. 6. Mean torques and powers from the set-point controller (SP) for both knee and ankle, with normative reference curves from human data [28]. Gray shaded area spans $\pm$ one standard deviation across simulated trials.

With the PV controller, we find that the across-subject mean RMSE is $4.93°$ for the ankle trajectory and $6.32°$ for the knee. The maximum RMSE is $8.59°$ for the ankle and $10.38°$ for the knee. The error is almost doubled with the SP controller. The across-subject mean RMSE is $8.83°$ for the ankle trajectory and $18.1°$ for the knee. The maximum RMSE is $13.0°$ for the ankle and $23.5°$ for the knee. Note that Figure 7 shows a typical source of error, which is an offset in the final ankle angle position of the human subject.

To contextualize these results, we also compute the RMSE between pairs of trajectories observed experimentally in each subject. The mean RMSE for the ankle and knee is reported in the third and fourth columns of Table II, respectively. The across-subject mean RMSE for the ankle is $2.72°$ and $5.15°$ for the knee, while the maximum is $3.60°$ for the ankle and $10.18°$ for the knee. Comparing these quantities with the RMSE between PV simulations and experimental trials, we observe that the mean error of the controller is $2.26°$ higher for the ankle and $1.27°$ higher for the knee. This suggests that the trajectories induced by the PV controller may be, for the most part, included in the natural variability of normative human sit-to-stand motion.

C. Rise Time

We define rise time as the time required to rise from 10% to 90% of maximum knee extension. The mean rise time for each subject is reported in the fourth column of Table III. The mean rise time of the set of simulations corresponding to each subjects' recorded parameters and initial conditions is in the second column of Table III for the PV controller, and the third column for the SP controller. The overall mean rise time of the PV simulation trials is 0.59 seconds and 0.37 seconds for the SP simulations. The mean rise time observed in the experiment is 0.72 seconds.

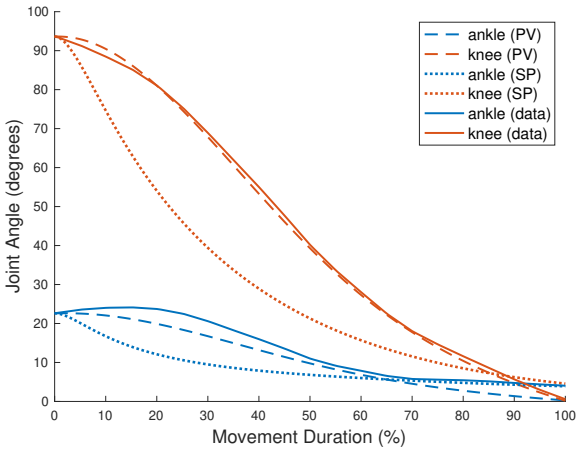

Fig. 7. Representative kinematics of prosthesis with SP and PV control, and corresponding kinematics from one trial. All sets of kinematic trajectories begin from the same initial condition. An ankle angle offset at standing, which is a typical source of error for the PV controller, can be observed. In contrast, the error of the SP controller is consistent throughout the trial.

TABLE II

KINEMATIC COMPARISON: MEAN RMSE BETWEEN EXPERIMENTAL TRIALS AND SIMULATIONS OF PV AND SP CONTROLLERS; MEAN INTRA-SUBJECT RMSE FOR EXPERIMENTAL DATA (IS)

Sub.	θ_1 PV	θ_2 PV	θ_1 SP	θ_2 SP	θ_1 IS	θ_2 IS
1	4.29°	6.17°	8.01°	16.6°	2.11°	4.59°
2	4.25°	3.04°	7.65°	18.7°	3.60°	4.89°
3	6.69°	7.19°	11.0°	23.5°	1.75°	3.32°
4	8.59°	3.34°	13.0°	23.0°	1.97°	3.94°
5	4.10°	8.12°	8.71°	15.9°	3.15°	3.97°
6	5.64°	5.46°	9.11°	18.1°	2.29°	3.28°
7	2.79°	5.40°	7.12°	16.7°	2.58°	2.51°
8	2.92°	6.69°	6.35°	11.4°	2.30°	7.43°
9	5.33°	10.38°	8.18°	19.4°	3.50°	6.38°
10	5.03°	7.45°	9.12°	18.1°	3.41°	10.18°

The rise times are of course dependent both on the controller gains and on the vertical force approximating the contribution of the sound-side. The downside of such a simplified model is that we cannot easily separate these effects. However, the results shown in Figure 7 suggest that acceleration is consistently scaled for the PV simulation and data, particularly when there is no observed joint hyper-extension. The SP controller, on the other hand, produces qualitatively different trajectories from human subject data.

VI. CONCLUSION

This paper presented a new mathematical model of amputees performing sit-to-stand, which explicitly represents only the amputated side while still accounting for the driving motion of the sound side. We have also designed the first phase-variable controller for sit-to-stand motion, using the thigh angle as the phase variable. In simulation, our results show that the controller can handle a range of realistic initial conditions and parameters and produces joint angle trajectories that are similar to those observed experimentally, and produces torques, powers, and rise times that are consistent with normative human sit-to-stand.

TABLE III

MEAN RISE TIMES (SECONDS) FOR PROSTHESIS SIMULATIONS AND HUMAN SUBJECT TRIALS

Subject	PV	SP	Experiment
1	0.59	0.34	0.95
2	0.58	0.40	1.06
3	0.60	0.35	1.01
4	0.56	0.39	0.60
5	0.47	0.38	0.73
6	0.58	0.39	0.54
7	0.97	0.38	0.50
8	0.55	0.40	0.71
9	0.62	0.34	0.67
10	0.45	0.35	0.43

As our controller is time-invariant, a possible benefit is giving the amputee control both over cycle progression and direction of motion. Data of subjects performing stand-to-sit motion show the same linear relationship between the phase variable and knee as in sit-to-stand, allowing us to apply the presented control method to stand-to-sit motion. It is also important to demonstrate in simulation that the controller can respond appropriately to changes in intent, or failures during sit-to-stand, such as sitting back down mid-motion.

The developed mathematical model for amputee sit-to-stand is also amenable to model-based formal verification techniques, which we plan to explore in future work. Furthermore, the presented controller merits further investigation on a real prosthesis in an experimental study with amputees, where we plan to measure symmetry between the torques produced on the sound side and the prosthetic side.

REFERENCES

[1] P. M. Dall and A. Kerr, "Frequency of the sit to stand task: An observational study of free-living adults," *Applied Ergonomics*, vol. 41, no. 1, pp. 58 – 61, 2010.

[2] P. O. Riley, M. L. Schenkman, R. W. Mann, and W. Hodge, "Mechanics of a constrained chair-rise," *Journal of Biomechanics*, vol. 24, no. 1, pp. 77 – 85, 1991.

[3] P. D. Holmes, S. M. Danforth, X.-Y. Fu, T. Y. Moore, and R. Vasudevan, "Characterizing the limits of human stability during motion: perturbative experiment validates a model-based approach for the sit-to-stand task," *Royal Society Open Science*, vol. 7, no. 1, p. 191410, 2020.

[4] P. O. Riley, D. E. Krebs, and R. A. Popat, "Biomechanical analysis of failed sit-to-stand," *IEEE Transactions on Rehabilitation Engineering*, vol. 5, no. 4, pp. 353–359, 1997.

[5] L. Nolan, A. Wit, K. Dudziński, A. Lees, M. Lake, and M. Wychowañski, "Adjustments in gait symmetry with walking speed in trans-femoral and trans-tibial amputees," *Gait & Posture*, vol. 17, no. 2, pp. 142 – 151, 2003.

[6] H. Burger, J. Kuželički, and Črt Marinček, "Transition from sitting to standing after trans-femoral amputation," *Prosthetics and Orthotics International*, vol. 29, no. 2, pp. 139–151, 2005. PMID: 16281723.

[7] R. Gailey, K. Allen, J. Castles, J. Kucharik, and M. Roeder, "Review of secondary physical conditions associated with lower-limb amputation and long-term prosthesis use," *Journal of Rehabilitation Research and Development*, vol. 45, no. 1, pp. 15–29, 2008.

[8] A. F. Azocar, L. M. Mooney, L. J. Hargrove, and E. J. Rouse, "Design and characterization of an open-source robotic leg prosthesis," in *2018 7th IEEE International Conference on Biomedical Robotics and Biomechatronics (Biorob)*, pp. 111–118, 2018.

[9] T. Elery, S. Rezazadeh, C. Nesler, and R. D. Gregg, "Design and validation of a powered knee-ankle prosthesis with high-torque, low-impedance actuators," *IEEE Trans. Robotics*, 2020.

[10] H. A. Varol, F. Sup, and M. Goldfarb, "Powered sit-to-stand and assistive stand-to-sit framework for a powered transfemoral prosthesis," in *2009 IEEE International Conference on Rehabilitation Robotics*, pp. 645–651, 2009.

[11] A. M. Simon, N. P. Fey, K. A. Ingraham, S. B. Finucane, E. G. Halsne, and L. J. Hargrove, "Improved weight-bearing symmetry for transfemoral amputees during standing up and sitting down with a powered knee-ankle prosthesis," *Archives of Physical Medicine and Rehabilitation*, vol. 97, no. 7, pp. 1100 – 1106, 2016.

[12] A. M. Simon, K. A. Ingraham, N. P. Fey, S. B. Finucane, R. D. Lipschutz, A. J. Young, and L. J. Hargrove, "Configuring a powered knee and ankle prosthesis for transfemoral amputees within five specific ambulation modes," *PloS one*, vol. 9, no. 6, p. e99387, 2014.

[13] D. Quintero, D. J. Villarreal, D. J. Lambert, S. Kapp, and R. D. Gregg, "Continuous-phase control of a powered knee–ankle prosthesis: Amputee experiments across speeds and inclines," *IEEE Transactions on Robotics*, vol. 34, no. 3, pp. 686–701, 2018.

[14] S. Rezazadeh, D. Quintero, N. Divekar, E. Reznick, L. Gray, and R. D. Gregg, "A phase variable approach for improved rhythmic and non-rhythmic control of a powered knee-ankle prosthesis," *IEEE Access*, vol. 7, pp. 109840–109855, 2019.

[15] T. Elery, S. Rezazadeh, E. Reznick, L. Gray, and R. D. Gregg, "Effects of a powered knee-ankle prosthesis on amputee hip compensations: A case series," *IEEE Transactions on Neural Systems and Rehabilitation Engineering*, 2020.

[16] R. Aissaoui and J. Dansereau, "Biomechanical analysis and modelling of sit to stand task: a literature review," in *IEEE International Conference on Systems, Man, and Cybernetics*, vol. 1, pp. 141–146 vol.1, 1999.

[17] H. Hemami and V. C. Jaswa, "On a three-link model of the dynamics of standing up and sitting down," *IEEE Transactions on Systems, Man, and Cybernetics*, vol. 8, no. 2, pp. 115–120, 1978.

[18] J. Kuželički, M. Žefran, H. Burger, and T. Bajd, "Synthesis of standing-up trajectories using dynamic optimization," *Gait & Posture*, vol. 21, no. 1, pp. 1 – 11, 2005.

[19] M. F. Bobbert, D. A. Kistemaker, M. A. Vaz, and M. Ackermann, "Searching for strategies to reduce the mechanical demands of the sit-to-stand task with a muscle-actuated optimal control model," *Clinical Biomechanics*, vol. 37, pp. 83–90, 2016.

[20] E. Reznick, K. Embry, R. Neuman, E. Bolivar-Nieto, N. P. Fey, and R. D. Gregg, "Lower-limb kinematics and kinetics during continuously varying human locomotion," *Scientific Data*, 2021. under review.

[21] A. Kralj, R. Jaeger, and M. Munih, "Analysis of standing up and sitting down in humans: Definitions and normative data presentation," *Journal of Biomechanics*, vol. 23, no. 11, pp. 1123 – 1138, 1990.

[22] M. Galli, V. Cimolin, M. Crivellini, and I. Campanini, "Quantitative analysis of sit to stand movement: Experimental set-up definition and application to healthy and hemiplegic adults," *Gait & Posture*, vol. 28, no. 1, pp. 80 – 85, 2008.

[23] D. A. Winter, *The Biomechanics and Motor Control of Human Gait: Normal, Elderly and Pathological*. Waterloo Biomechanics, 01 1991.

[24] E. Caruthers, J. A. Thompson, A. Chaudhari, L. Schmitt, T. Best, K. Saul, and R. Siston, "Muscle forces and their contributions to vertical and horizontal acceleration of the center of mass during sit-to-stand transfer in young, healthy adults.," *Journal of applied biomechanics*, vol. 32 5, pp. 487–503, 2016.

[25] R. M. Murray, S. S. Sastry, and L. Zexiang, *A Mathematical Introduction to Robotic Manipulation*. USA: CRC Press, Inc., 1st ed., 1994.

[26] C. Chevallereau, J. W. Grizzle, and C.-L. Shih, "Asymptotically stable walking of a five-link underactuated 3-d bipedal robot," *Trans. Rob.*, vol. 25, p. 37–50, Feb. 2009.

[27] P. de Leva, "Adjustments to zatsiorsky-seluyanov's segment inertia parameters," *Journal of Biomechanics*, vol. 29, no. 9, pp. 1223 – 1230, 1996.

[28] M. Roebroeck, C. Doorenbosch, J. Harlaar, R. Jacobs, and G. Lankhorst, "Biomechanics and muscular activity during sit-to-stand transfer," *Clinical Biomechanics*, vol. 9, no. 4, pp. 235 – 244, 1994.

[29] S. T. Hurley, D. J. Rutherford, and C. Hubley-Kozey, "The effect of age and seat height on sit-to-stand transfer biomechanics and muscle activation," *Physical & Occupational Therapy In Geriatrics*, vol. 34, no. 4, pp. 169–185, 2016.